Available online at www.sciencedirect.com

ScienceDirect

Procedia Computer Science 225 (2023) 3425–3431

Procedia Computer Science

www.elsevier.com/locate/procedia

27th International Conference on Knowledge-Based and Intelligent Information & Engineering Systems (KES 2023)

Fuzzy deconvolution of neuronal events in Functional Magnetic Resonance Imaging

Alejandro Veloz[a,b,∗], Wael El-Deredy[a,b], Alejandro Weinstein[a,b], Juan Zamora[c], Claudio Moraga[d], Daniele Marinazzo[e]

[a] *School of Biomedical Engineering, Universidad de Valparaíso, Gral. Cruz 222, Valparaíso 2340000, Chile.*
[b] *Centro de Investigación y Desarrollo en Ingeniería en Salud, Universidad de Valparaíso, Gral. Cruz 222, Valparaíso 2340000, Chile.*
[c] *Instituto de Estadística, Pontificia Universidad Católica de Valparaíso, Avenida Brasil 2830, Valparaíso 2340000, Chile.*
[d] *TU Dortmund University, 44269 Dortmund, Germany.*
[e] *Department of Data Analysis, Ghent University, 2 Henri Dunantlaan, B-9000 Ghent, Belgium.*

Abstract

The variability in the shape of the Blood Oxygenation Level Dependent (BOLD) response, as measured in Functional Magnetic Resonance Imaging (fMRI), can introduce significant uncertainty and inaccuracies in estimating brain connectivity and detecting brain activity. To address this issue, this paper proposes a fuzzy method that offers enhanced robustness in dealing with the inherent uncertainty associated with the brain's response in fMRI data.

The results obtained from simulated data demonstrate that the proposed fuzzy method is capable of effectively handling deviations of the Hemodynamic Response Function from its canonical shape, providing promising potential for improving the accuracy and reliability of fMRI analyses.

Keywords: Fuzzy Hemodynamic Response Function; Functional MRI; Neural events deconvolution

1. Introduction

Functional Magnetic Resonance Imaging (fMRI) plays an important role in elucidating brain function. Most fMRI analyses relies on the assumption of that Blood Oxygenation Level Dependent (BOLD) responses measured on fMRI which are evoked by neural events are explained by a LTI (Linear Time-Invariant) model. Thus, at voxel $v \in \{1,\ldots,V\}$, the measured fMRI signal, denoted by $\mathbf{y}_v$, is related to neural activity represented by the binary signal $\mathbf{x}_v$, through the convolution sum of $\mathbf{x}_v$ and an impulse response $\mathbf{h}$, that is referred to as Hemodynamic Response Function (HRF).

∗ Corresponding author. Tel.: +56-32-2603662.
E-mail address: alejandro.veloz@uv.cl

1877-0509 © 2023 The Authors. Published by Elsevier B.V.

10.1016/j.procs.2023.10.337

Therefore, the measured BOLD response satisfies the following model:

$$\mathbf{y}_v = \mathbf{h} * \mathbf{x}_v + \varepsilon_v, \tag{1}$$

where $\mathbf{y}_v$, $\mathbf{h}$, $\mathbf{x}_v$, and ε_v are all N-dimensional vectors of real numbers. The term ε_v is the noise, and $*$ denotes the convolution operator.

Deconvolution of neural events from fMRI data assumes that the data is generated by a Linear Time-Invariant (LTI) process, as described in Eq. (1). This estimation of $\mathbf{x}_v$ is typically done with the assumption that the Hemodynamic Response Function (HRF), denoted as $\mathbf{h}$, is known and fixed. One important application of deconvolution is to enhance the signal-to-noise ratio of raw fMRI signals, which is often very low, before conducting connectivity analysis [17]. However, the HRF exhibits significant variability in its characteristic parameters, such as time-to-peak, response delay, dispersion, and amplitude, across different brain areas, age groups, and in response to structural or functional changes following brain damage [9, 14, 16]. As a result, many conventional methods used for fMRI analyses, which rely on rigid assumptions about the shape of the HRF, may not account for individual variations, leading to inaccuracies in the detection of brain activity [14, 17].

The approach presented in this work builds upon the fuzzy model of the BOLD response, as proposed in [15], to address the deconvolution problem of neural events. The proposed approach establishes a relationship between the BOLD signal and neural activity through a convolution sum of a sequence of binary values representing neural events and a fuzzy Hemodynamic Response Function (HRF). The fuzzy HRF is a discrete-time sequence of fuzzy sets that is designed to capture the known variability of the HRF, taking into account the numerous uncertainties and unknowns in the biophysical and biochemical mechanisms that transform the activity of a small group of neurons into the BOLD response.

The structure of this paper is as follows: Section 2 outlines the fuzzy model of the BOLD response and the proposed deconvolution method. Section 3 presents results obtained with simulated fMRI data. Finally, Section 4 provides a discussion and conclusion of the findings presented in this article.

2. Deconvolution of neural events using a fuzzy model of the BOLD response

2.1. The fuzzy model of the BOLD response

The fuzzy model of the BOLD response at a given voxel is given by:

$$\widetilde{\mathbf{y}} = \widetilde{\mathbf{H}}\mathbf{x} + \varepsilon, \tag{2}$$

where $\mathbf{x}$ and ε are two N-dimensional vectors of real numbers representing neural activity and noise, respectively. Parameter N is the number of time points acquired in during the fMRI experiment. The terms $\widetilde{\mathbf{y}} \in \mathscr{F}(\mathbb{R})^N$ and $\widetilde{\mathbf{H}} \in \mathscr{F}(\mathbb{R})^{N\times N}$ are a N-dimensional vector and a $N \times N$ Toeplitz matrix of fuzzy numbers with triangular shape, respectively. The term $\mathscr{F}(\mathbb{R})$ represents the space of fuzzy numbers with triangular shape defined over the real line. The term $\widetilde{\mathbf{y}}$ represents the fuzzy BOLD response and has elements denoted by $\widetilde{y}_i$, where i is the sample index taking values $i = 1, \ldots, N$. The term $\widetilde{\mathbf{H}}$ is the fuzzy HRF $\widetilde{\mathbf{h}} \in \mathscr{F}(\mathbb{R})^N$ presented in matrix form according to the Toeplitz structure. And the term $\widetilde{h}_i$ denotes an element of the fuzzy HRF. For the sake of simplicity we omitted subscript v used in Eq. (1).

The fuzzy HRF is a vector of fuzzy numbers that codifies, according to their membership degrees, the level of possibility that the HRF takes certain value at a given time instant [15]. An instance of the fuzzy HRF is shown in Fig. 1. Membership degrees are coded using gray-scale, where darker colors indicate a higher membership degree. Each element of the fuzzy HRF is characterized by a triangular fuzzy number $\widetilde{h}_i \in \mathscr{F}(\mathbb{R})$ whose left, center and right membership function parameters are determined in such a way that a set of plausible HRFs are covered by a membership degree of at least $\alpha^* \in [0,1]$ (α^* level is an user-selected parameter). The set of plausible HRFs $\mathscr{I} = \{\mathbf{h}_1, \ldots, \mathbf{h}_{|\mathscr{I}|}\}$ ($|\mathscr{I}|$ denotes its cardinality) are chosen to be consistent with the empirical evidence. This evidence suggests that the time-to-peak (TTP) is in the range between 4 and 8 seconds and that the *full width at half maximum* (FWHM) is in the range between two and five seconds [8, 9, 10, 14]. The set of curves $\mathscr{I}$ was generated using the double γ-variate HRF formula proposed by Glover [7]. This formula depends on the set of parameters $\{\tau_1, \tau_2, \delta_1, \delta_2, c\}$. A grid search over the Cartesian product space of the intervals $\tau_1 = [2, 10]$ and $\tau_2 = [8, 15]$ is used to select the HRF instances that match with the TTP and FWHM shape criterion.

The left, center and right parameters of the i-th fuzzy HRF element are denoted by h_i^ℓ, h_i^c, and h_i^r, respectively. Let $\mathbf{h}^c$ be the vector containing h_i^c parameters that corresponds to the HRF trajectory with the highest level of possibility (represented in red line in Fig. 1). The $\mathbf{h}^c$ term is determined by solving a variable selection problem using the ℓ_1 regression approach. The BOLD forward model of Eq. (1) was reformulated assuming that the observed BOLD signal is explained by the weighted sum of the set of plausible HRFs $\mathscr{I}$, i.e.

$$\mathbf{y} = \mathbf{h}_1 * \mathbf{x}_1 + \cdots + \mathbf{h}_{|\mathscr{I}|} * \mathbf{x}_{|\mathscr{I}|} + \varepsilon = \sum_{j=1}^{|\mathscr{I}|} \mathbf{H}_j \mathbf{x}_j + \varepsilon, \tag{3}$$

where $\mathbf{h}_j \in \mathscr{I}$ is a plausible HRF and $\mathbf{H}_j$ denotes its corresponding Toeplitz matrix form. Thus, $\mathbf{h}^c$ is determined according to:

$$\mathbf{h}^c = \mathbf{h}_{j^*} \Leftrightarrow j^* = \arg \max_{j=1,\dots,|\mathscr{I}|} \sum_{j=1}^{|\mathscr{I}|} \|\mathbf{x}_j^*\|_1,$$

where $\mathbf{x}_j^*$ are optimal vectors obtained by solving:

$$\mathbf{x}_1^*, \dots, \mathbf{x}_{|\mathscr{I}|}^* = \arg \min_{\mathbf{x}_1,\dots,\mathbf{x}_{|\mathscr{I}|}} \{\|\mathbf{y} - \sum_{j=1}^{|\mathscr{I}|} \mathbf{H}_j \mathbf{x}_j\|_2^2 + \lambda_c \sum_{j=1}^{|\mathscr{I}|} \|\mathbf{x}_j\|_1\}, \quad \lambda_c > 0, \tag{4}$$

where λ_c is a regularization parameter that is chosen experimentally. In this work, Eq. (4) was solved using the subgradient method (see [1] for details about the method).

The h_i^ℓ and h_i^r parameters are the left and right parameters of the corresponding fuzzy HRF element $\widetilde{h}_i$, respectively. These elements are arranged in vectors $\mathbf{h}^\ell$ and $\mathbf{h}^r$, respectively.

Let $[\widetilde{h}_i]_{\alpha^*} = [\widetilde{h}_i^L(\alpha^*), \widetilde{h}_i^U(\alpha^*)]$ be the α^* level of $\widetilde{h}_i$, with $\widetilde{h}_i^L(\alpha^*)$ and $\widetilde{h}_i^U(\alpha^*)$ being the lower and upper limits of such interval, respectively, and let h_{ij} be the i-th element of the j-th HRF contained in $\mathscr{I}$. The interval $[\widetilde{h}_i]_{\alpha^*}$ is determined according to:

$$[\widetilde{h}_i]_{\alpha^*} = \left[\min_j \; h_{ij}, \; \max_j \; h_{ij} \right]. \tag{5}$$

Thus, assuming fuzzy numbers with triangular shape, the h_i^ℓ and h_i^r parameters can be computed as:

$$h_i^\ell = \frac{-\alpha^* h_i^c + \widetilde{h}_i^L(\alpha^*)}{1-\alpha^*}, \tag{6}$$

$$h_i^r = \frac{-\alpha^* h_i^c + \widetilde{h}_i^U(\alpha^*)}{1-\alpha^*}. \tag{7}$$

2.2. Deconvolution of neural activity using LR fuzzy numbers

The deconvolution of neuronal events $\mathbf{x}$ from Eq. (2) is an inverse problem that can be expressed according to:

$$\min_{\mathbf{x}} \{d(\widetilde{\mathbf{y}}, \widetilde{\mathbf{H}}\mathbf{x})^2 + \lambda \|\mathbf{x}\|_1\}, \quad \lambda > 0, \tag{8}$$

where $d : \mathbb{R}^N \to \mathbb{R}$ is a fidelity term that expresses the similarity between the measured signal $\widetilde{\mathbf{y}}$ and the signal predicted by the model $\widetilde{\mathbf{H}}\mathbf{x}$. λ is an user-defined regularization parameter that is determined experimentally.

To estimate the neural activity by minimizing Eq. (8), this work resorts to the LR representation of fuzzy numbers with triangular shape [11]. This is a well known approach to perform arithmetic operations between fuzzy numbers. Let $\widetilde{p} = \langle p^\ell, p^c, p^r \rangle$ and $\widetilde{q} = \langle q^\ell, q^c, q^r \rangle$ be two fuzzy numbers with triangular shape, where (p^ℓ, p^c, p^r) and (q^ℓ, q^c, q^r) denotes the left, center and right parameters of triangular membership functions of $\widetilde{p}$ and $\widetilde{q}$, respectively. According to the notation typically utilized in LR fuzzy numbers, the sum and scalar multiplication between triangular LR fuzzy numbers is defined according to $\widetilde{p} + \widetilde{q} = \langle p^\ell + q^\ell, p^c + q^c, p^r + q^r \rangle$ and $a\widetilde{p} = \langle ap^\ell, ap^c, ap^r \rangle$ if $a > 0$ and $a\widetilde{p} = \langle ap^r, ap^c, ap^\ell \rangle$ if $a < 0$, respectively, where $a \in \mathbb{R}$.

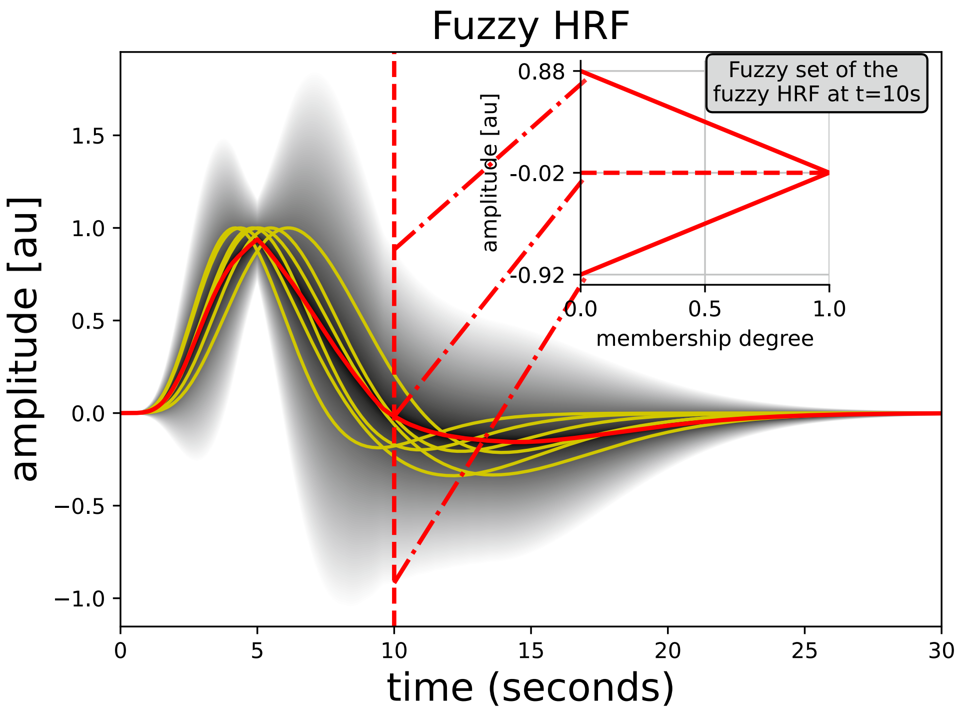

Fig. 1. Fuzzy haemodynamic response function. Each time point is mapped into a fuzzy set that represents possible values of the HRF. Membership values are represented by the gray-scale. Specific HRF instances, shown in yellow, were generated using the γ-variate model of [7]. The HRF instance plotted in red corresponds to the HRF that is established as the HRF trajectory with the highest level of membership.

Under the LR approach for fuzzy numbers, Eq. (2) can be expressed according to:

$$\begin{bmatrix} \langle y_1^\ell, y_1^c, y_1^r \rangle \\ \vdots \\ \langle y_N^\ell, y_N^c, y_N^r \rangle \end{bmatrix} = \begin{bmatrix} \langle h_{11}^\ell, h_{11}^c, h_{11}^r \rangle & \dots & \langle h_{1N}^\ell, h_{1N}^c, h_{1N}^r \rangle \\ \vdots & \ddots & \vdots \\ \langle h_{N1}^\ell, h_{N1}^c, h_{N1}^r \rangle & \dots & \langle h_{NN}^\ell, h_{NN}^c, h_{NN}^r \rangle \end{bmatrix} \mathbf{x} + \varepsilon, \tag{9}$$

where $\widetilde{h}_{ij} = \langle h_{ij}^\ell, h_{ij}^c, h_{ij}^r \rangle$ corresponds to the ij fuzzy number of the fuzzy HRF Toeplitz matrix. Eq. (9) can be also written as:

$$\langle \mathbf{y}^\ell, \mathbf{y}^c, \mathbf{y}^r \rangle = \langle \mathbf{H}^\ell \mathbf{x}, \mathbf{H}^c \mathbf{x}, \mathbf{H}^r \mathbf{x} \rangle + \varepsilon, \tag{10}$$

where $\mathbf{H}^\ell$, $\mathbf{H}^c$, and $\mathbf{H}^r$ are matrices that contains the left, center, and right parameters of the fuzzy HRF Toeplitz matrix, respectively.

To solve Eq. (8) under the LR approach, we adopted the Alternating Direction Method of Multipliers (ADMM) that is widely used in sparse estimation literature [2]. To do this, the similarity criterion proposed by Diamond in the context of fuzzy regression (see [6, 5, 18]) is employed as the fidelity term d that is needed to evaluate Eq. (8). Thus, the objective function to be minimized is the following:

$$\min_{\mathbf{x}} \{ \|\mathbf{y}^\ell - \mathbf{H}^\ell \mathbf{x}\|_2^2 + \|\mathbf{y}^c - \mathbf{H}^c \mathbf{x}\|_2^2 + \|\mathbf{y}^r - \mathbf{H}^r \mathbf{x}\|^2 + \lambda \|\mathbf{x}\|_1 \}, \quad \lambda > 0. \tag{11}$$

Under the ADMM optimization framework, Eq. (11) is rewritten as:

$$\begin{aligned} &\min_{\mathbf{x}} \{ \|\mathbf{y}^\ell - \mathbf{H}^\ell \mathbf{x}\|_2^2 + \|\mathbf{y}^c - \mathbf{H}^c \mathbf{x}\|_2^2 + \|\mathbf{y}^r - \mathbf{H}^r \mathbf{x}\|^2 + \lambda \|\mathbf{z}\|_1 \} \\ &\text{s.t.} \quad \mathbf{x} - \mathbf{z} = 0. \end{aligned} \tag{12}$$

ADMM requires to form the augmented Lagrangian of the above problem, yielding:

$$\begin{aligned} L_\rho(\mathbf{x},\mathbf{u},\mathbf{z}) =& \|\mathbf{y}^\ell - \mathbf{H}^\ell\mathbf{x}\|_2^2 + \|\mathbf{y}^c - \mathbf{H}^c\mathbf{x}\|_2^2 + \|\mathbf{y}^r - \mathbf{H}^r\mathbf{x}\|^2 \\ &+ \lambda\|\mathbf{z}\|_1 + (1/\rho)\mathbf{u}'(\mathbf{x}-\mathbf{z}) + (\rho/2)\|\mathbf{x}-\mathbf{z}\|_2^2. \end{aligned} \tag{13}$$

ADMM consists of the iterations:

$$\mathbf{x}^{k+1} = \arg\min_{\mathbf{x}} L_\rho(\mathbf{x},\mathbf{u}^k,\mathbf{z}^k) \tag{14}$$

$$\mathbf{z}^{k+1} = \arg\min_{\mathbf{z}} L_\rho(\mathbf{x}^k,\mathbf{u}^k,\mathbf{z}) \tag{15}$$

$$\mathbf{u}^{k+1} = \mathbf{u}^k + \rho(\mathbf{x}^{k+1} - \mathbf{z}^{k+1}) \tag{16}$$

Eq. (14) can be solved taking the gradient $L_\rho(\mathbf{x},\mathbf{u}^k,\mathbf{z}^k)$ with respect to $\mathbf{x}$:

$$\nabla_{\mathbf{x}} L_\rho(\mathbf{x},\mathbf{u}^k,\mathbf{z}^k) = -\mathbf{H}^{\ell\top}\mathbf{y}^\ell + \mathbf{H}^{\ell\top}\mathbf{H}^\ell\mathbf{x} - \mathbf{H}^{c\top}\mathbf{y}^c + \mathbf{H}^{c\top}\mathbf{H}^c\mathbf{x} - \mathbf{H}^{r\top}\mathbf{y}^r + \mathbf{H}^{r\top}\mathbf{H}^r\mathbf{x} + \rho(\mathbf{x}-\mathbf{z}+\mathbf{u}) = 0. \tag{17}$$

Thus, iteration of Eq. (14) can be obtained by:

$$\mathbf{x}^{k+1} = (\mathbf{H}^{\ell\top}\mathbf{H}^\ell + \mathbf{H}^{c\top}\mathbf{H}^c + \mathbf{H}^{r\top}\mathbf{H}^r + \rho I)^{-1}(\mathbf{H}^{\ell\top}\mathbf{y}^\ell + \mathbf{H}^{c\top}\mathbf{y}^c + \mathbf{H}^{r\top}\mathbf{y}^r + \rho(\mathbf{z}^k - \mathbf{u}^k)). \tag{18}$$

Similarly, iteration of Eq. (15) can be obtained by the soft-thresholding operator:

$$\mathbf{z}^{k+1} = S_{\lambda/\rho}(\mathbf{x}^{k+1} - \mathbf{u}^k). \tag{19}$$

It must be noted that multiplication of a LR fuzzy number and a scalar involves exchanging its left and right parameters depending on the sign of the scalar, i.e. the corresponding element of $\mathbf{x}$ of Eq. (9). Therefore, before calculating $\mathbf{x}^{k+1}$ using Eq. (18), at coordinate i,j the elements of $\mathbf{H}^\ell$ and $\mathbf{H}^r$, denoted by h_{ij}^ℓ and h_{ij}^r, respectively, are determined by the following rule:

$$\{h_{ij}^\ell, h_{ij}^r\} = \begin{cases} \{h_{ij}^\ell, h_{ij}^r\} & x_i^k > 0 \\ \{h_{ij}^r, h_{ij}^\ell\} & \text{otherwise} \end{cases} \tag{20}$$

3. Experimental evaluation

We conducted an accuracy evaluation of our method using synthetic BOLD data generated based on the standard Linear Time-Invariant (LTI) model (Eq.(1)). The purpose of this experiment was to investigate the performance of our method when the assumed shape of the underlying Hemodynamic Response Function (HRF) used for data generation deviates significantly from the deconvolution model being employed. As a comparison, we also evaluated the performance of the Lasso method, which is commonly used for deconvolution in previous studies[3, 4, 12, 13], and utilizes the Glover's canonical HRF as the expected BOLD response model (Eq. (1)).

To generate the BOLD signals, we chose a sampling time (Time of Repetition, TR) of one second. Neural response signals were generated with five individual neural responses of one TR duration. The onsets of individual neural responses were randomly distributed in time, allowing the BOLD signal to return to its baseline before the next neural response onset. Gaussian noise with zero-mean and standard deviation σ_{noise} was added to contaminate the BOLD signals, with the σ_{noise} value computed to achieve a Signal-to-Noise Ratio (SNR) of 0.5, using the expression $\text{SNR} = \frac{\sigma_{\text{signal}}}{\sigma_{\text{noise}}}$.

To assess the performance of the methods, we computed the Mean Squared Error (MSE) and the area under the Receiver-Characteristic-Operating Curve (ROC) generated by thresholding the solutions obtained from both our proposed method and the Lasso.

We generated ten thousand datasets, and for each dataset, we generated BOLD signal instances using the Glover HRF [7] with varying times-to-peak (TTP) parameters of 5, 6, 7, and 8 seconds, and Full-Width-Half-Maximum (FWHM) parameters of 3, 4, 5, and 6 seconds. Figure 2 illustrates the MSE and the area under the ROC curves as a function of the TTP and FWHM parameters, obtained from the ten thousand experimental runs.

4. Discussion and conclusion

The main objective of this study was to develop a novel framework for the analysis of functional magnetic resonance imaging (fMRI) data, capable of accommodating deviations in the shape of the hemodynamic response function

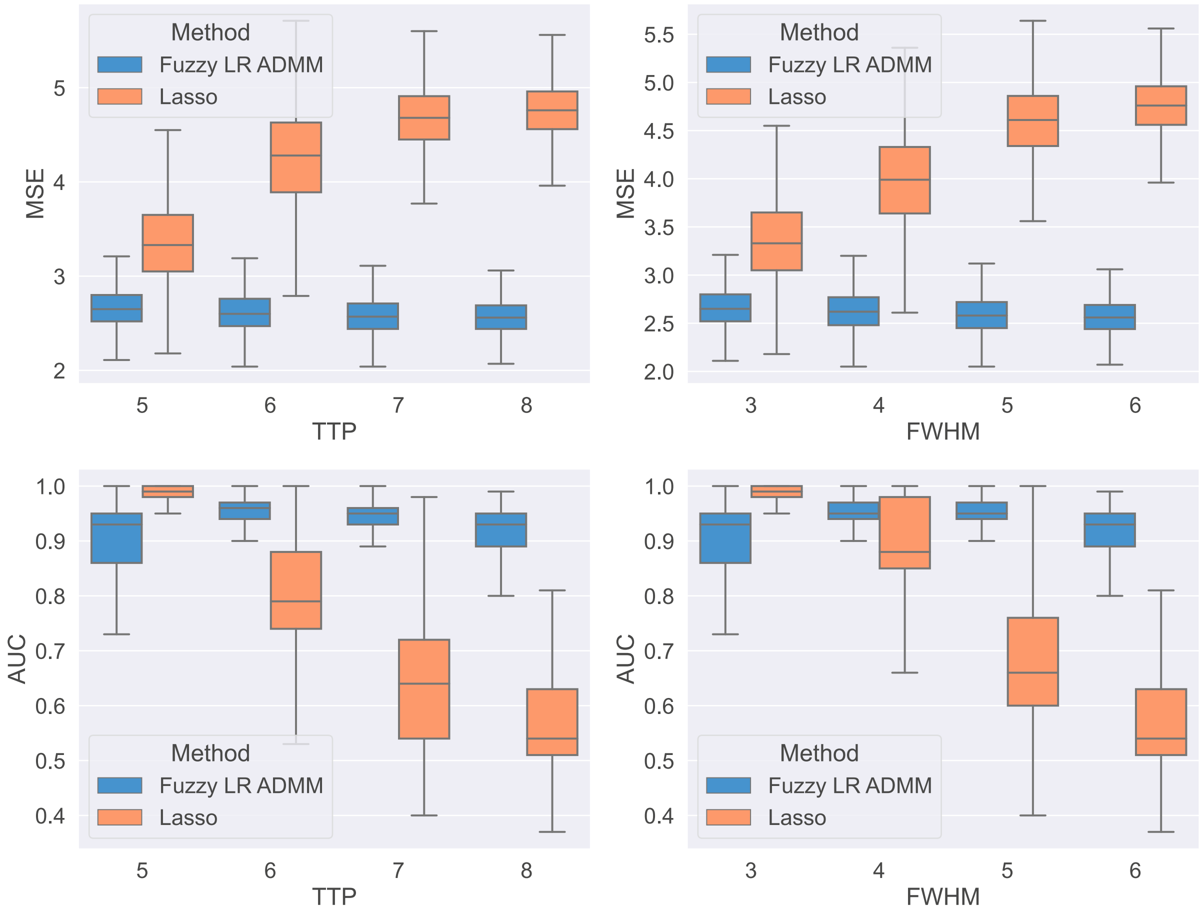

Fig. 2. Mean Squared Error (MSE) (top panel) and area under the ROC curves (bottom panel) as a function of the TTP and FWHM parameters obtained from ten thousand experimental runs.

(HRF) from its canonical form. To assess the performance of our method, we conducted a comprehensive evaluation on synthetic data.

As depicted in Figure 2, our proposed method exhibited robust performance across a range of simulated scenarios. Even when the time-to-peak (TTP) and full-width at half-maximum (FWHM) parameters of the underlying HRF used to generate the data varied across different seconds, our method consistently yielded accurate results. This indicates that our approach is relatively insensitive to variations in the HRF characteristics assumed in the model, making it a reliable tool for handling deviations from the canonical HRF shape.

In contrast, the conventional Lasso approach, which assumes a fixed model of the HRF, demonstrated performance degradation when the assumed HRF shape did not match the characteristics of the data. This highlights the limitations of assuming a fixed HRF model in situations where the true HRF deviates from the canonical shape. Our proposed method, on the other hand, proved to be more flexible and adaptable to varying HRF shapes, making it a promising approach for analyzing fMRI data with non-canonical HRF characteristics.

Future research directions include investigating the performance of our method on real-world, in vivo fMRI data. Specifically, our approach may be particularly suitable for analyzing resting state fMRI data of patients affected by health conditions that alter the hemodynamic characteristics of the brain, such as brain tumors. In such cases, the conventional fMRI analysis based on the canonical HRF may not be accurate enough, and our method could potentially provide more reliable and interpretable results in identifying brain network connections [17].

Despite its promising performance, our proposed method has some limitations. One important constraint is that it currently only allows for the use of fuzzy numbers of the left-right (LR) type. This requires the assumption of a particular shape of fuzzy numbers, such as triangular shapes, to achieve a linear transition of membership degrees between neighboring HRF trajectories. However, there may be cases where other non-linear fuzzy number shapes, such as Gaussian shapes, could provide a better fit or capture the underlying uncertainties more accurately. Using α-cut-based representations, which do not impose any specific shape on fuzzy numbers, could potentially overcome this limitation and provide more flexibility in modeling the uncertainties associated with HRF trajectories.

In conclusion, our proposed framework for analyzing fMRI data with non-canonical HRF shapes has demonstrated robust performance on synthetic data, showing its potential for real-world applications in neuroimaging research. Further investigations and refinements are needed to fully exploit the advantages of this approach, including evaluating its performance on real fMRI data and exploring alternative representations of fuzzy numbers to enhance its flexibility and applicability in various scenarios.

Acknowledgements

This work was supported by FONDECYT iniciación 11201046 and FONDECYT 1201822 research grants.

References

[1] Aggarwal, C., 2020. Linear Algebra and Optimization for Machine Learning. Springer.
[2] Boyd, S., Parikh, N., Chu, E., Peleato, B., Eckstein, J., 2011. Distributed optimization and statistical learning via the alternating direction method of multipliers. Foundations and Trends in Machine Learning 3, 1–122.
[3] Caballero-Gaudes, C., Petridou, N., Dryden, I., Bai, L., Francis, S., Gowland, P., 2011. Detection and characterization of single-trial fMRI BOLD responses: paradigm free mapping. Human Brain Mapping 32, 1400–1418.
[4] Caballero-Gaudes, C., Petridou, N., Francis, S., Dryden, I., Gowland, P., 2013. Paradigm free mapping with sparse regression automatically detects single-trial fMRI BOLD responses. Human Brain Mapping 39, 501–518.
[5] Chen, L., Hsueh, C., 2009. Fuzzy regression models using the least-squares method based on the concept of distance. IEEE Transactions on Fuzzy Systems 17, 1259 –1272.
[6] Diamond, P., 1988. Fuzzy least squares. Information Sciences 46, 141–157.
[7] Glover, G., 1999. Deconvolution of impulse response in event-related BOLD fMRI. Neuroimage 9, 416–419.
[8] Handwerker, D., Gazzaley, A., Inglis, B., D'Esposito, M., 2007. Reducing vascular variability of fMRI data across aging populations using a breathholding task. Hum Brain Mapp 28, 846–859.
[9] Handwerker, D., Gonzalez-Castillo, J., D'Esposito, M., Bandettini, P., 2012. The continuing challenge of understanding and modeling hemodynamic variation in fMRI. Neuroimage 62, 1017–1023.
[10] Handwerker, D., Ollinger, J., D'Esposito, M., 2004. Variation of BOLD hemodynamic responses across subjects and brain regions and their effects on statistical analyses. Neuroimage 21, 1639–1651.
[11] Hanss, M., 2005. Applied Fuzzy Arithmetic. Springer-Verlag.
[12] Hernandez-Garcia, L., Ulfarsson, M., 2011. Neuronal event detection in fMRI time series using iterative deconvolution techniques. Magnetic Resonance Imaging 29, 353–364.
[13] Karahanoğlu, F., Caballero-Gaudes, C., Lazeyras, F., Van De Ville, D., 2013. Total activation: fMRI deconvolution through spatio-temporal regularization. Neuroimage 73, 121–134.
[14] Lindquist, M., Loh, J., Atlas, L., Wager, T., 2009. Modeling the hemodynamic response function in fMRI: Efficiency, bias and mis-modeling. Neuroimage 45, S187–S198.
[15] Veloz, A., Moraga, C., Weinstein, A., Hernández-García, L., Chabert, S., Salas, R., Riveros, R., Bennett, C., Allende, H., 2020. Fuzzy General Linear Modeling for Functional Magnetic Resonance Imaging analysis. IEEE Transactions on Fuzzy Systems 28, 100–111.
[16] Villanueva-Meyer, J., Mabray, M., Cha, S., 2017. Current clinical brain tumor imaging. Neurosurgery 81, 397–415.
[17] Wang, Y., David, O., Hu, X., Deshpande, G., 2017. Can Patel's τ accurately estimate directionality of connections in brain networks from fMRI? Magnetic Resonance in Medicine 78, 2003–2010.
[18] Yoon, J., Choi, S., 2013. Fuzzy least squares estimation with new fuzzy operations. Advances in Intelligent Systems and Computing 190, 193–202.